NJC

Cadmium sulfide quantum dots stabilized by aromatic amino acids for visible light-induced photocatalytic degradation of organic dyes

Jie Zhang, Yuming Guo,* Hui Fang, Weili Jia, Han Li, Lin Yang and Kui Wang

In the present study, three aromatic amino acids including histidine, phenylalanine, and tryptophan were used as stabilizing agents for the preparation of cadmium sulfide quantum dots through a facile one-pot method under mild conditions. The as-prepared cadmium sulfide quantum dots exhibited strong visible light absorption and green photoluminescence. In addition, by using quantum dots as catalysts, rhodamine B and methylene blue could be photocatalytically degraded through the mediation of the photo-generated hydroxyl radicals under visible light irradiation. Furthermore, the photocatalytic performance of the quantum dots did not exhibit a significant decrease after five cycles of photocatalytic reaction. These results suggested that the cadmium sulfide quantum dots prepared in this study might be used as potential photocatalysts to efficiently treat organic pollutants under visible light irradiation.

Introduction

Recently, on account of the exceptional properties including a relatively narrow band gap, size-dependent electronic, and excellent optical properties, cadmium sulfide (CdS) nanoscaled materials especially quantum dots (QDs) are extensively used in various fields.[1–10] Compared with UV-light-responsive photocatalysts, *e.g.* TiO$_2$, visible-light-responsive photocatalysts can directly use a larger part of the solar spectrum, offering a desirable way to solve environmental issues, such as CdS, Ag$_3$PO$_4$, and boron carbides.[11–15] Unfortunately, the preparation of stable CdS QDs remains a difficult task because of the ultra-high surface energy and the corresponding undesirable agglomeration. Therefore, it is still a great challenge to prepare the relatively stable and well-dispersed CdS QDs under mild conditions. Previously, synthetic organic surfactants were frequently selected to be used as stabilizing agents for the preparation of stable inorganic nanomaterials, *e.g.* QDs.[16–20] However, the sophisticated synthesis procedures and the potential toxicities of the organic surfactants seriously limit the corresponding applications. From previous studies, the functional groups of the amino acids could interact with transition metal ions to form stable complexes.[21–24] Consequently, amino acids might be selected as the potential stabilizing agents for the preparation of stable QDs. Several

studies reported the preparation of stable CdS QDs using different amino acids as stabilizing agents.[25–28] However, heretofore the aromatic amino acids are seldom used as stabilizing agents for the preparation of stable CdS QDs in aqueous media.

Currently, with the development of human society, large amounts of synthetic organic dyes are widely applied in textile, leather tanning, paper production, food technology, light harvesting arrays, and photo-electrochemical cells, *etc.*[29–32] Because of their large scale production and extensive use, colored wastewaters containing toxic and non-biodegradable synthetic organic dyes are discharged into natural aquatic environments posing a serious ecological risk. Therefore, it is an imperative and challenging task to explore the suitable approaches to efficiently treat these synthetic organic dyes. From the studies, photocatalytic degradation was considered as a superior method to treat synthetic organic dyes, in which semiconductor nanoscaled materials were considered as potential photocatalyst candidates.[33–36] Unfortunately, most of the existing semiconductor photocatalysts can only photocatalytically degrade the organic dyes under UV light irradiation. However, the content of UV light in the sunlight spectral is less than 5%, and in contrast, visible light whose wavelength ranges from 400 to 700 nm accounts for 43%.[37] So the practical applications of the existing semiconductor photocatalysts are severely restricted. Therefore, it is still a great challenge to explore the appropriate photocatalysts to degrade synthetic organic dyes efficiently under visible light irradiation.

In the current study, three aromatic amino acids, histidine (His), phenylalanine (Phe), and tryptophan (Trp), are selected to be used as efficient stabilizing agents for the preparation of stable CdS QDs through a facile one-pot aqueous method.

Collaborative Innovation Center of Henan Province for Green Manufacturing of Fine Chemicals, Key Laboratory of Green Chemical Media and Reactions, Ministry of Education, School of Chemistry and Chemical Engineering, Henan Normal University, Xinxiang 453007, P. R. China. E-mail: guoyuming@gmail.com; Fax: +86-373-3328507; Tel: +86-373-3329255

The as-prepared QDs showed good photocatalytic activities and recycling stability for the degradation of synthetic organic dyes under visible light irradiation through the mediation of photo-generated hydroxyl radicals ($^\bullet$OH).

Experimental

Materials

All the chemicals were of analytical grade and were used without any further purification. His, Phe, Trp, cadmium chloride (CdCl$_2$·2.5H$_2$O), thioacetamide (TAA), rhodamine B (RhB), methylene blue (MB), terephthalic acid (TPA), vitamin C, sodium hydroxide (NaOH), and hydrochloride acid (HCl) were purchased from China National Pharmaceutical Group Corp. Double distilled water (DD water) was used throughout the investigations.

Preparation of CdS QDs

In the current study, for the facile one-pot preparation of the amino acid stabilized CdS QDs, 0.12 mmol of amino acid and 0.06 mmol of cadmium chloride were dissolved into 25 mL of DD water and the pH value of the solution was adjusted to 10.0 using 1 M NaOH or HCl aqueous solution. Then the solution was incubated at 25 °C for 12 h under moderate stirring for the complete interaction between Cd^{2+} and amino acid. Subsequently, 25 mL of 3 mM TAA aqueous solution was added dropwise into the above mixed solution. Afterwards, the reaction system was refluxed for 1 h at 100 °C under moderate stirring and the color of the reaction system changed to yellow. Finally, the yellow dispersion was centrifuged under refrigeration, washed with DD water and absolute ethanol for several times, and dried under vacuum conditions at 40 °C for 24 h. The as-prepared yellow products were denoted as His-QDs, Phe-QDs, and Trp-QDs. For comparison, a control experiment was performed under the same conditions for the preparation of bulk CdS in the absence of amino acids.

Characterization

The morphologies of the as-prepared CdS QDs were characterized using a JEOL JEL-2010 high resolution transmission electron microscope (HR-TEM) at an accelerating voltage of 200 kV. The size distribution analysis of the CdS QDs was performed using the log normal function from 100 particles in an arbitrarily chosen area. Powder X-ray diffraction (XRD) patterns of the samples were recorded on BrukerAXS D8 Advanced diffractometer with a graphite monochromatized Cu Kα radiation source (λ = 1.5406 Å). A scanning rate of 0.05 deg s^{-1} was applied to record the pattern in the 2θ range of 20–70°. The Fourier transform infrared (FT-IR) spectra were recorded on a Bio-Rad FTS-40 FT-IR spectrometer in the wavenumber range of 4000–400 cm^{-1}. The UV-visible absorption and photoluminescence (PL) spectra were recorded on a Lambda-17 UV-vis Spectrophotometer and a Cary Eclipse Fluorescence spectrophotometer, respectively.

Evaluation of photocatalytic activity

For the photocatalytic activity evaluation, 30 mg of the CdS QDs were dispersed into 24 mL of DD water through ultrasonication for 30 min. Then 6 mL of RhB or MB aqueous solution (250 ppm) was introduced into CdS QD suspension. The suspension was magnetically stirred in the dark for *ca.* 60 min to achieve the adsorption/desorption equilibrium between organic dyes and CdS QDs. Subsequently, the photocatalytic reaction system was exposed to the irradiation of 500 W xenon lamp to perform the photocatalytic degradation of organic dyes under magnetic stirring. At the regular intervals, 4 mL of the suspension was withdrawn from the reaction vessel and centrifuged to remove the photocatalysts. The concentration of organic dyes in the supernatant was determined by UV-visible absorption spectroscopy at 554 nm for RhB and 664 nm for MB. The photocatalytic degradation rate was calculated using eqn (1):

$$\text{Photodegradation rate \%} = (A_0 - A) \times 100\%/A_0 \qquad (1)$$

where A_0 is the initial absorbance of organic dyes and A is the final absorbance after treatment with photocatalysts for certain periods of time.

For comparison, the photocatalytic activities of the bulk CdS and the commercially available TiO$_2$ (Degussa P25) were also evaluated under the same conditions.

Determination of [Cd^{2+}]

The concentrations of Cd^{2+} before and after photocatalytic reaction were determined using the inductively coupled plasma-mass spectrometer (ICP-MS, ELAN DRC-e, Perkin-Elmer Sciex). To determine [Cd^{2+}] in the system after five cycles of photocatalytic reaction, the mixture after each cycle of reaction was ultracentrifuged to remove any possible solid samples completely. All the supernatants from each cycle of reaction were combined and analyzed by ICP-MS.

Analysis of photo-generated $^\bullet$OH

With the assistance of TPA, the formation of the photo-generated $^\bullet$OH radical on the surface of the photo-irradiated CdS QDs was detected *in situ* by a fluorimetric assay. In this approach, TPA can efficiently react with a photo-generated $^\bullet$OH radical formed at the water/catalyst interface to produce a highly fluorescent product, 2-hydroxyterephthalic acid (HTPA), which can emit a strong fluorescence signal at 425 nm.[38–40] The fluorescence intensity of the HTPA is directly proportional to the amount of photo-generated $^\bullet$OH radicals in the system. This technique is rapid, sensitive, and specific and therefore extensively used in many fields for the facile and sensitive detection of the $^\bullet$OH radical generated in aqueous media.[39–41] The detection conditions were absolutely identical to those used in the evaluation of photocatalytic activity except the replacement of the aqueous solution of RhB with the aqueous solution of TPA. The photo-irradiation was employed and the suspension was withdrawn from the reaction vessel every 20 min. Subsequently, the suspension was centrifuged to remove the photocatalysts. Then, the fluorescence intensity of the supernatant at 425 nm upon excitation at a wavelength of 315 nm was recorded to represent the amount of photo-generated $^\bullet$OH radicals.

Confirmation of the photocatalytic degradation mechanism

In order to further confirm the mediation effect of the photo-generated •OH radicals on the photocatalytic degradation of RhB in the presence of CdS QDs, additional 0.1 mg mL^{-1} vitamin C aqueous solution was introduced into the photocatalysis reaction suspension to perform the photocatalytic degradation of RhB under the identical conditions to the photocatalytic activity evaluation experiments. The photocatalytic activities in the presence of vitamin C were compared with those of the evaluation experiments in the absence of vitamin C.

Results and discussion

Characterization of the CdS QDs

In this study, the XRD patterns were recorded to determine the polymorphs of the CdS QDs. From the results displayed in Fig. 1, all the CdS QDs exhibit similar XRD patterns, the three diffraction peaks located at the 2θ values of $26.75°$, $44.05°$ and $52.11°$ can be assigned to the (111), (220) and (311) planes of the cubic CdS phase (JCPDF 75-0581), respectively. This result clearly reveals that the CdS QDs are successfully prepared under the stabilization of His, Phe, Trp. The broadness of the diffraction peaks can be attributed to the ultrasmall sizes of the CdS QDs.

The size and morphologies of the CdS QDs were analyzed by HR-TEM. From the results shown in Fig. 2a1–c1, all the CdS QDs exhibit similar spherical-like morphologies. From the size distribution analysis (Fig. 2a2–c2), the mean diameters of the His-QDs (4.72 nm), Phe-QDs (6.47 nm), and Trp-QDs (5.25 nm) are different from each other, also different from the CdS QDs under the stabilization of other amino acids.[27,42] This suggests that it is possible to adjust the diameter of QDs through the careful selection of the stabilizing agents. Furthermore, from the inset of Fig. a1–c1, the lattice fringe spacings of the as-prepared QDs are 0.3360 nm, 0.3357 nm, and 0.3372 nm, which correspond to the (111) plane of the cubic CdS and confirms the formation of the cubic CdS under the stabilization of the aromatic amino acids. In addition, the bulk CdS prepared in the absence of amino acids is
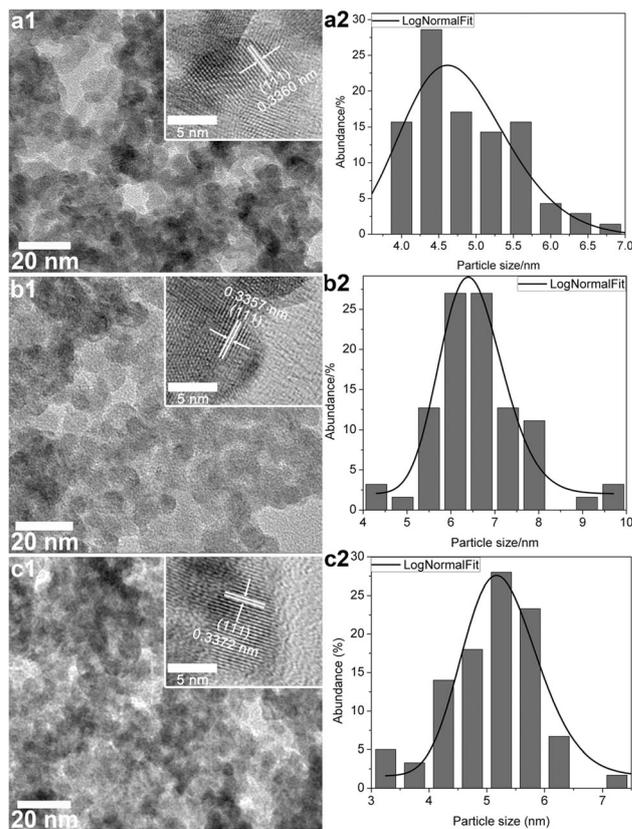
Fig. 2 (a1–c1) HR-TEM images of the CdS QDs stabilized by His, Phe, and Trp; (a2–c2) Particle size distributions of His-QDs, Phe-QDs, and Trp-QDs.

much bigger and exhibits serious agglomeration (data not shown), indicating the crucial roles of aromatic amino acids in the efficient regulation of the size, morphology, and dispersion of the CdS QDs.

Fig. 3 shows the FT-IR spectra of the CdS QDs and the bulk counterpart. Compared with the bulk CdS, the stretching bending band of the carbonyl group of aromatic amino acids
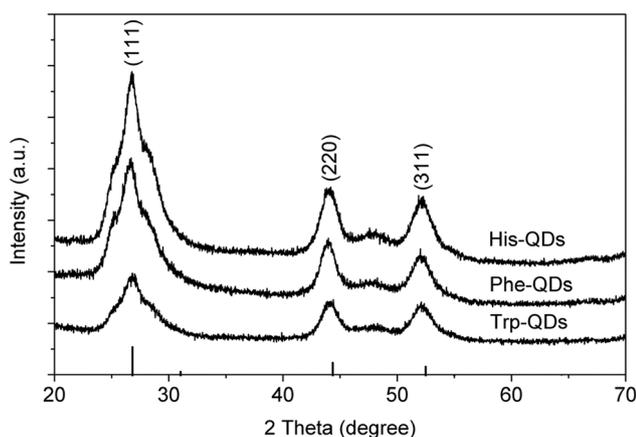
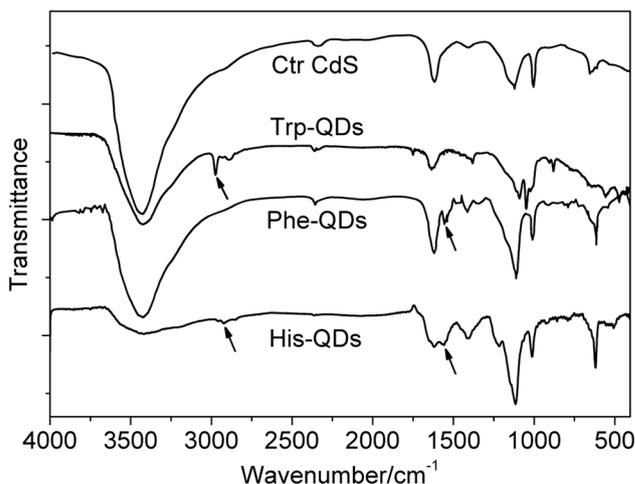**Fig. 1** XRD patterns of the CdS QDs stabilized by different aromatic amino acids.

Fig. 3 FT-IR spectra of the CdS QDs stabilized by His, Phe, and Trp and the bulk CdS prepared from the control experiment.
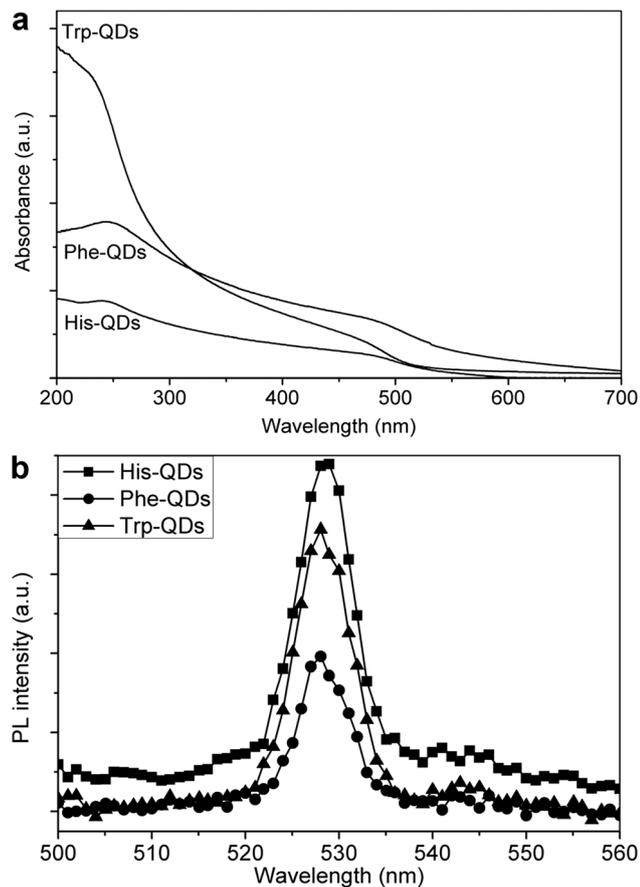
Fig. 4 (a) UV-visible absorption spectra of the as-prepared CdS QDs; (b) PL spectra of the as-prepared CdS QDs under 202 nm excitation.

at 1550–1580 cm^{-1} and the stretching vibration band of CH of amino acids at 2910–2920 cm^{-1} can be found in the spectra of the CdS QDs. However, the absorption intensities of these bands decrease obviously compared with the pure amino acids. This indicates that there are certain interactions between the CdS QDs and the functional groups of amino acids. It should be these interactions that contribute to the stability and dispersity of the CdS QDs.

The photo-properties of the CdS QDs were determined, including the UV-visible absorption and the PL spectra. From the UV-visible absorption spectra shown in Fig. 4a, all the CdS QDs exhibit a broad absorption band from 200 to 550 nm, indicating the strong photoabsorption properties in the UV and visible light region. In addition, from the PL spectra of the CdS QDs shown in Fig. 4b, all the CdS QDs exhibit a strong green emission peak at around 528 nm when excited under light at a wavelength of 202 nm. This can be attributed to the recombination of the charge carriers within surface states.[27]

Photocatalytic degradation activity of the CdS QDs on RhB under visible light irradiation

On account of the good UV-visible photoabsorption properties of the as-prepared CdS QDs, the potential application of the CdS QDs to photocatalytically degrade the synthetic organic
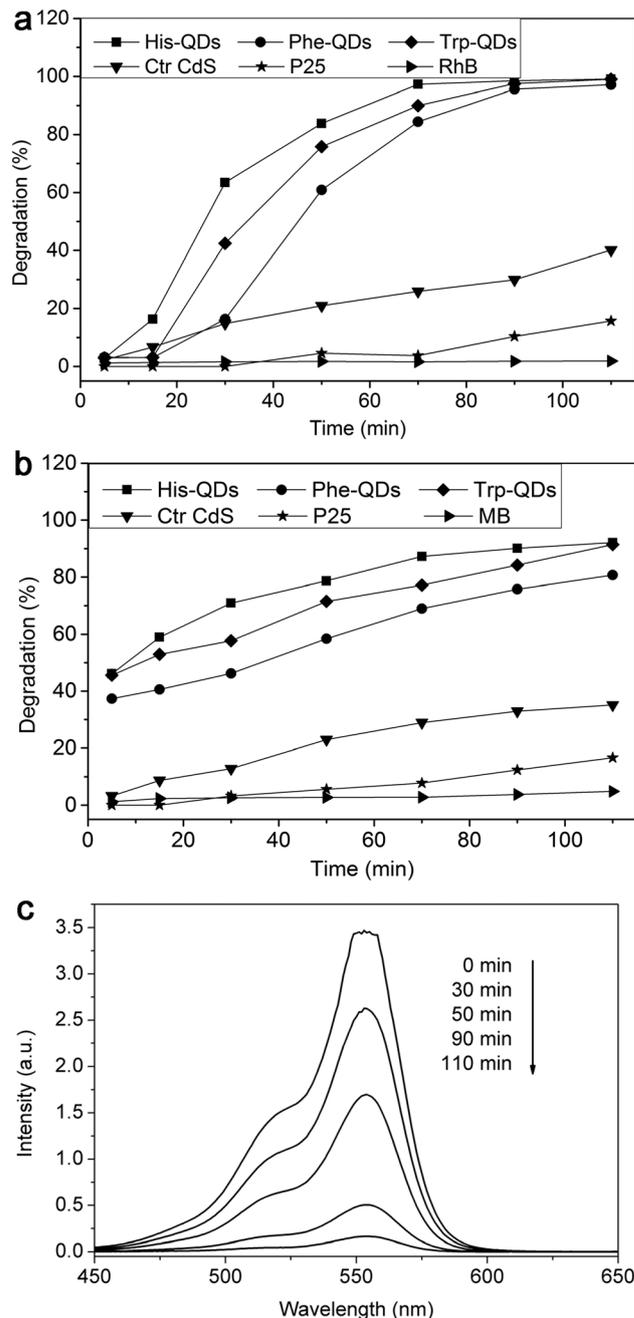
Fig. 5 Photocatalytic degradation of (a) RhB and (b) MB in the presence of the CdS QDs under visible light irradiation. (c) The UV-visible absorption spectra of RhB after being photocatalytically degraded by His-QDs for different times.

dyes under visible light irradiation were evaluated. From the results shown in Fig. 5a, compared with the reference samples including bulk CdS and commercial P25, the as-prepared CdS QDs show much stronger photocatalytic degradation activities on RhB. Moreover, from Fig. 5b, the as-prepared CdS QDs also exhibit the efficient photocatalytic degradation activities on MB. The photocatalytic degradation spectra of RhB after treatment with His-QDs for different periods of time are selected to be shown in Fig. 5b to confirm the gradual degradation of RhB.

From the results, the photocatalytic activities of the CdS QDs prepared in this study are found to be much stronger than the results of the previous reports.[27,42] The sequence of the photo-catalytic effects of the samples on RhB and MB is His-QDs > Trp-QDs > Phe-QDs, which is well correlated with those of the mean diameters and the PL intensities. This correlation might be attributed to the recombination rates of the photo-generated electron–hole pairs on the QDs. Generally, the lower the PL intensity, the lower the recombination rates, and the higher the photocatalytic activities of semiconductors.[43]

The recycling stabilities of the CdS QDs during the photocatalytic reaction

The recycling stability of a certain photocatalyst is critical for its practical application. Therefore the recycling stabilities of the as-prepared CdS QDs on the photocatalytic degradation of RhB were evaluated. From the results shown in Fig. 6a–c, the photocatalytic activities of the CdS QDs do not show an obvious decrease after five cycles of the photocatalytic reaction, revealing their excellent recycling stabilities. In addition, the morphologies of the CdS QDs do not exhibit the obvious changes after five cycle degradation reactions (Fig. 6d–f). From the ICP-MS analysis, after five cycle degradation reactions, the overall concentration of Cd^{2+} in the reaction system is 0.04 mg L^{-1}, similar to the original concentration (0.03 mg L^{-1}), indicating the stability of the QDs during the photocatalytic reaction process. These results propose that the CdS QDs prepared in this study might be used as the useful photocatalysts to degrade synthetic organic dyes under visible light irradiation. More importantly, as the potential novel

photocatalysts, the CdS QDs can be reused for many cycles without a great decrease in photocatalytic activity during the reactions, exhibiting their potential in the practical and long-time applications.

Photocatalytic degradation mechanism of organic dyes in the presence of CdS QDs

From previous studies, the hydroxyl radical ($^{\bullet}OH$), superoxide (O_2^-), and hydrogen peroxide (H_2O_2) might be the key active intermediates in the photocatalytic degradation of synthetic organic dyes.[44,45] Therefore, the photo-generated $^{\bullet}OH$ formed on the surface of photo-illuminated CdS QDs was determined using the PL intensity as the indicator. From the linear fitting plots of PL intensity at 425 nm against irradiation time shown in Fig. 7a, the PL intensities increase gradually with the increase of the irradiation period, suggesting the successive generation of $^{\bullet}OH$ on the surface of the CdS QDs during the irradiation process. The PL intensity under UV irradiation in TPA solutions increases linearly against time. Consequently, it can be inferred that $^{\bullet}OH$ radicals produced at the surface of QDs are in proportion to the light irradiation time obeying zero-order reaction rate kinetics. The formation rate of the $^{\bullet}OH$
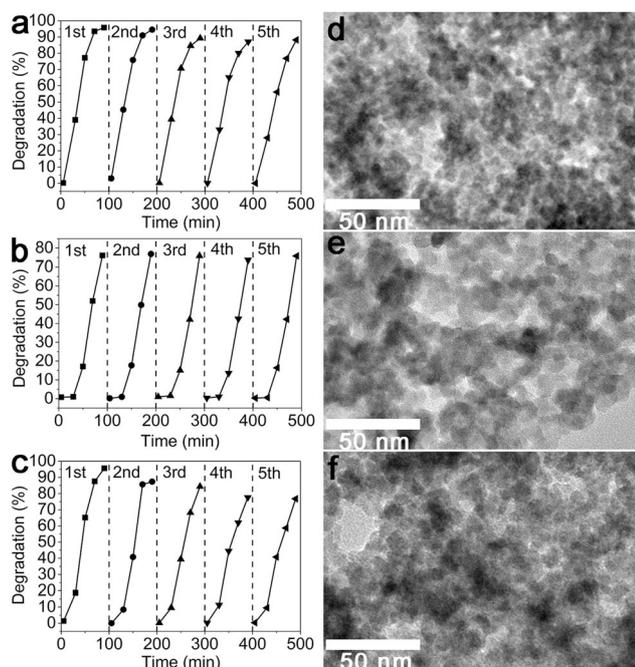

Fig. 6 The recycling of the as-prepared CdS QDs on the photocatalytic degradation of RhB under visible light irradiation. (a) His-QDs; (b) Phe-QDs; (c) Trp-QDs. TEM images of the CdS QDs after five cycles of photocatalytic reactions. (d) His-QDs; (e) Phe-QDs; (f) Trp-QDs.
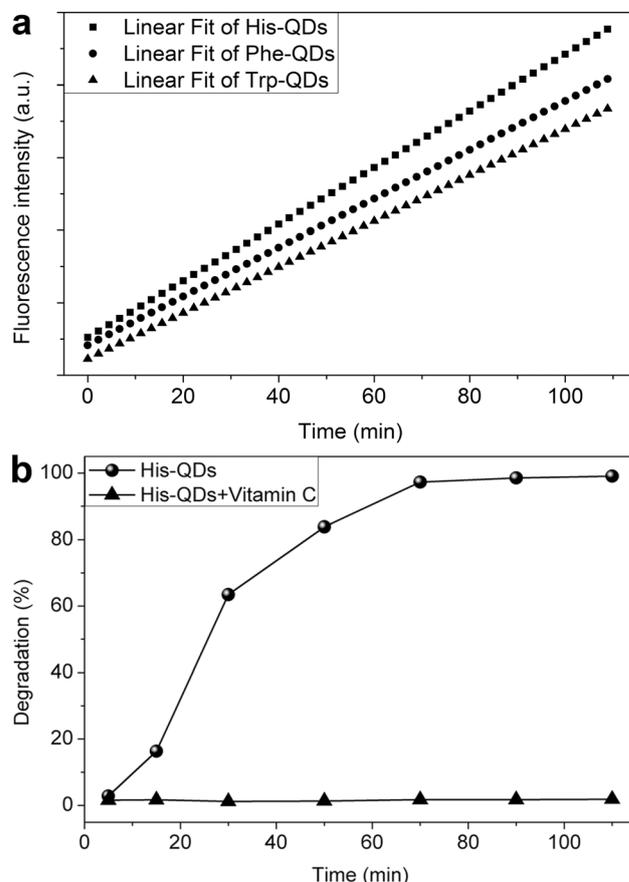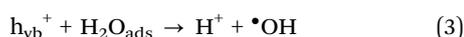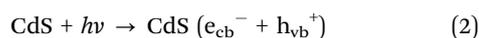

Fig. 7 (a) Linear fitting curves of the induced PL intensities at 426 nm against irradiation time for TPA on the as-prepared CdS QDs. (b) The photodegradation of RhB in the presence of His-QDs and His-QDs + vitamin C.

radicals could be expressed by the slope of fitting lines shown in Fig. 7a. The slopes of the fitting lines of His-QDS, Trp-QDs, and Phe-QDs are 1.9498, 1.6833, and 1.5836, respectively. It can be easily seen that the formation rates of $^{\bullet}$OH radicals on the surface of different QDs are significantly different. The sequence of the formation rates of $^{\bullet}$OH radicals is His-QDS > Trp-QDs > Phe-QDs, which agrees well with the sequence of the photocatalytic activities.

Based on these results, the possible photocatalytic degradation mechanism of RhB in the presence of the CdS QDs under visible light irradiation is proposed as follows. Firstly, the photons with the energy higher than that of the band gap of the CdS QDs are absorbed on the surface of QDs. This results in the excitation of the electrons from the valence band (vb) to the conduction band (cb), which can produce a hole (h_{vb}^{+}) at the valence band edge and an electron (e_{cb}^{-}) in the conduction band of the QDs (eqn (2)). Secondly, h_{vb}^{+} and e_{cb}^{-} can react with water or hydroxyl groups absorbed on the surface of QDs to generate highly reactive $^{\bullet}$OH radicals (eqn (3) and (4)). Finally, the $^{\bullet}$OH radicals can react with the RhB molecules absorbed on the surface of QDs to perform the photodegradation of the RhB (eqn (5)):

$$CdS + h\nu \rightarrow CdS\ (e_{cb}^{-} + h_{vb}^{+}) \qquad (2)$$

$$h_{vb}^{+} + H_2O_{ads} \rightarrow H^{+} + {}^{\bullet}OH \qquad (3)$$

$$h_{vb}^{+} + OH^{-} \rightarrow {}^{\bullet}OH \qquad (4)$$

$${}^{\bullet}OH + dye_{ads} \rightarrow degradation\ of\ the\ dye \qquad (5)$$

In addition, in order to further confirm this proposed mechanism, vitamin C, a commonly used hydroxyl radical scavenger, was introduced into the photocatalytic reaction suspension to perform the photocatalytic degradation of RhB. From the result shown in Fig. 7b, the photocatalytic degradation activity of RhB in the presence of the mixture of vitamin C and His-QDs decreases significantly. This can be attributed to the scavenging of photo-generated $^{\bullet}$OH on the surface of QDs by vitamin C. This further confirms that the photocatalytic degradation of RhB by the QDs is really mediated by the photo-generated $^{\bullet}$OH formed on the surface of QDs.

Conclusions

In summary, using three different aromatic amino acids as stabilizers, stable CdS QDs were successfully prepared through a facile one-pot method under mild conditions. The as-prepared CdS QDs exhibited different properties, including different diameters and photo-properties. In addition, through the mediation of photo-generated $^{\bullet}$OH, the CdS QDs showed different photo-catalytic activities and good recycling stability to degrade synthetic organic dyes under visible light irradiation, implying the potential application in the treatment of the organic pollutants in wastewater. More importantly, the results suggest that the properties and the corresponding applications of the CdS QDs might be effectively adjusted through the careful selection of the stabilizing agents. This strategy might be potentially extended to prepare other inorganic nanomaterials with desirable properties and applications.

Notes and references

1 I. Coropceanu and M. G. Bawendi, *Nano Lett.*, 2014, **14**, 4097–4101.

2 C. Eley, T. Li, F. Liao, S. M. Fairclough, J. M. Smith, G. Smith and S. C. E. Tsang, *Angew. Chem., Int. Ed.*, 2014, **53**, 7838–7842.

3 S. Ghosh, A. Datta, N. Biswas, A. Datta and A. Saha, *RSC Adv.*, 2013, **3**, 14406–14412.

4 S. Ghosh, A. Datta and A. Saha, *Colloids Surf., A*, 2010, **355**, 130–138.

5 Y. Guo, J. Wang, Z. Tao, F. Dong, K. Wang, X. Ma, P. Yang, P. Hu, Y. Xu and L. Yang, *CrystEngComm*, 2012, **14**, 1185–1188.

6 Y. Guo, J. Wang, L. Yang, J. Zhang, K. Jiang, W. Li, L. Wang and L. Jiang, *CrystEngComm*, 2011, **13**, 5045–5048.

7 Y. Liao, J. Zhang, W. Liu, W. Que, X. Yin, D. Zhang, L. Tang, W. He, Z. Zhong and H. Zhang, *Nano Energy*, 2015, **11**, 88–95.

8 A. Priyam, S. Ghosh, S. C. Bhattacharya and A. Saha, *J. Colloid Interface Sci.*, 2009, **333**, 195–201.

9 S. Saha, G. Das, J. Thote and R. Banerjee, *J. Am. Chem. Soc.*, 2014, **136**, 14845–14851.

10 G. J. Supran, K. W. Song, G. W. Hwang, R. E. Correa, J. Scherer, E. A. Dauler, Y. Shirasaki, M. G. Bawendi and V. Bulović, *Adv. Mater.*, 2015, **27**, 1437–1442.

11 S. Ghosh, N. A. Kouamé, L. Ramos, S. Remita, A. Dazzi, A. Deniset-Besseau, P. Beaunier, F. Goubard, P.-H. Aubert and H. Remita, *Nat. Mater.*, 2015, **14**, 505–511.

12 J. Liu, S. Wen, Y. Hou, F. Zuo, G. J. Beran and P. Feng, *Angew. Chem., Int. Ed.*, 2013, **52**, 3241–3245.

13 E. Grabowska, A. Zaleska, S. Sorgues, M. Kunst, A. Etcheberry, C. Colbeau-Justin and H. Remita, *J. Phys. Chem. C*, 2013, **117**, 1955–1962.

14 Q. Li, B. Guo, J. Yu, J. Ran, B. Zhang, H. Yan and J. R. Gong, *J. Am. Chem. Soc.*, 2011, **133**, 10878–10884.

15 B. Zheng, X. Wang, C. Liu, K. Tan, Z. Xie and L. Zheng, *J. Mater. Chem. A*, 2013, **1**, 12635–12640.

16 Y. Duan, X. Liu, L. Han, S. Asahina, D. Xu, Y. Cao, Y. Yao and S. Che, *J. Am. Chem. Soc.*, 2014, **136**, 7193–7196.

17 L. Yuwen, B. Bao, G. Liu, J. Tian, H. Lu, Z. Luo, X. Zhu, F. Boey, H. Zhang and L. Wang, *Small*, 2011, **7**, 1456–1463.

18 J. W. Krumpfer, T. Schuster, M. Klapper and K. Müllen, *Nano Today*, 2013, **8**, 417–438.

19 S. Mourdikoudis and L. M. Liz-Marzán, *Chem. Mater.*, 2013, **25**, 1465–1476.

20 C. P. Joshi and T. P. Bigioni, *Langmuir*, 2014, **30**, 13837–13843.

21 J. Chin, S. S. Lee, K. J. Lee, S. Park and D. H. Kim, *Nature*, 1999, **401**, 254–257.

22 B.-O. David, C. Gerald, R. Nagaraja, B. Nick and L. Edward, *Eur. J. Biochem.*, 2001, **268**, 42–48.

23 A. V. Davis and T. V. O'Halloran, *Nat. Chem. Biol.*, 2008, **4**, 148–151.

24 J. M. Slocik, J. T. Moore and D. W. Wright, *Nano Lett.*, 2002, **2**, 169–173.

25 X. Cao, C. M. Li, H. Bao, Q. Bao and H. Dong, *Chem. Mater.*, 2007, **19**, 3773–3779.

26 A. Chatterjee, A. Priyam, S. C. Bhattacharya and A. Saha, *J. Lumin.*, 2007, **126**, 764–770.

27 Y. Guo, L. Jiang, L. Wang, X. Shi, Q. Fang, L. Yang, F. Dong and C. Shan, *Mater. Lett.*, 2012, **74**, 26–29.

28 Y. Guo, X. Shi, J. Zhang, Q. Fang, L. Yang, F. Dong and K. Wang, *Mater. Lett.*, 2012, **86**, 146–149.

29 I. Grčić, S. Papić, D. Mesec, N. Koprivanac and D. Vujević, *J. Photochem. Photobiol., A*, 2014, **273**, 49–58.

30 Q. Cao, R. Che and N. Chen, *Chem. Commun.*, 2014, **50**, 4931–4933.

31 W. Fan, W. Gao, C. Zhang, W. W. Tjiu, J. Pan and T. Liu, *J. Mater. Chem.*, 2012, **22**, 25108–25115.

32 X. Zhou, G. Liu, J. Yu and W. Fan, *J. Mater. Chem.*, 2012, **22**, 21337–21354.

33 H. Kisch, *Angew. Chem., Int. Ed.*, 2013, **52**, 812–847.

34 X. Lang, W. Ma, C. Chen, H. Ji and J. Zhao, *Acc. Chem. Res.*, 2014, **47**, 355–363.

35 V. Rajendran, A. König, K. S. Rabe and C. M. Niemeyer, *Small*, 2010, **6**, 2035–2040.

36 G. Zhang, G. Kim and W. Choi, *Energy Environ. Sci.*, 2014, **7**, 954–966.

37 Y. Liu, G. Chen, C. Zhou, Y. Hu, D. Fu, J. Liu and Q. Wang, *J. Hazard. Mater.*, 2011, **190**, 75–80.

38 B. I. Ipe, M. Lehnig and C. M. Niemeyer, *Small*, 2005, **1**, 706–709.

39 X. Yu, J. Yu, B. Cheng and B. Huang, *Chem. – Eur. J.*, 2009, **15**, 6731–6739.

40 W. Zhao, Y. Sun and F. N. Castellano, *J. Am. Chem. Soc.*, 2008, **130**, 12566–12567.

41 J. Yu, W. Wang, B. Cheng and B.-L. Su, *J. Phys. Chem. C*, 2009, **113**, 6743–6750.

42 Y. Guo, L. Wang, L. Yang, J. Zhang, L. Jiang and X. Ma, *Mater. Lett.*, 2011, **65**, 486–489.

43 J. Yu, H. Yu, B. Cheng, X. Zhao, J. C. Yu and W. Ho, *J. Phys. Chem. B*, 2003, **107**, 13871–13879.

44 M. Mehrjouei, S. Müller and D. Möller, *Chem. Eng. J.*, 2015, **263**, 209–219.

45 J. Xiao, Y. Xie and H. Cao, *Chemosphere*, 2015, **121**, 1–17.